Nat. Hazards Earth Syst. Sci., 23, 1355–1369, 2023
https://doi.org/10.5194/nhess-23-1355-2023

Natural Hazards and Earth System Sciences
Open Access
EGU

Grain size modulates volcanic ash retention on crop foliage and potential yield loss

Noa Ligot[1], **Patrick Bogaert**[1], **Sébastien Biass**[2], **Guillaume Lobet**[3,4], **and Pierre Delmelle**[1]

[1]Environmental Sciences, Earth and Life Institute, UCLouvain, Louvain-la-Neuve, Belgium
[2]Department of Earth Sciences, University of Geneva, Geneva, Switzerland
[3]Agricultural Sciences, Earth and Life Institute, UCLouvain, Louvain-la-Neuve, Belgium
[4]Agrosphere Institute, IBG-3, Forschungszentrum Jülich, Jülich, Germany

Correspondence: Noa Ligot (noa.ligot@uclouvain.be)

Received: 23 July 2022 – Discussion started: 31 August 2022
Revised: 3 March 2023 – Accepted: 15 March 2023 – Published: 11 April 2023

Abstract. Ashfall from volcanic eruptions endangers crop production and food security while jeopardising agricultural livelihoods. As populations in the vicinity of volcanoes continue to grow, strategies to reduce volcanic risks to and impacts on crops are increasingly needed. Current models of crop vulnerability to ash are limited. They also rely solely on ash thickness (or loading) as the hazard intensity metric and fail to reproduce the complex interplay of other volcanic and non-volcanic factors that drive impact. Amongst these, ash retention on crop leaves affects photosynthesis and is ultimately responsible for widespread damage to crops. In this context, we carried out greenhouse experiments to assess how ash grain size, leaf pubescence, and humidity conditions at leaf surfaces influence the retention of ash (defined as the percentage of foliar cover coated with ash) in tomato and chilli pepper plants, two crop types commonly grown in volcanic regions. For a fixed ash mass load ($\sim 570\,g\,m^{-2}$), we found that ash retention decreases exponentially with increasing grain size and is enhanced when leaves are pubescent (such as in tomato plants) or when their surfaces are wet. Assuming that leaf area index (LAI) diminishes with ash retention in tomato and chilli pepper plants, we derived a new expression for predicting potential crop yield loss after an ashfall event. We suggest that the measurement of crop LAI in ash-affected areas may serve as an impact metric. Our study demonstrates that quantitative insights into crop vulnerability can be gained rapidly from controlled experiments. We advocate this approach to broaden our understanding of ash–plant interactions and to validate the use of remote sensing methods for assessing crop damage and recovery at various spatial and time scales after an eruption.

1 Introduction

The livelihood and food security of hundreds of millions of people living near and on volcanoes intricately depend on agriculture (Small and Naumann, 2001; Brown et al., 2015). However, farming activities in these regions are exposed to short-term, i.e. usually less than 1 year, negative impacts of volcanic eruptions, an issue amplified by the expanding population living under volcanic risk (Brown et al., 2015; Freire et al., 2019). Where cropping activity dominates (for example in Indonesia), widespread damage to agriculture during eruptive activity arises from crop exposure to ashfall (e.g. Burket et al., 1980; de Guzman, 2005; Tampubolon et al., 2018), causing adverse effects that range from temporary perturbations in leaf physiology to irreversible mechanical damage (Eggler, 1948; Blong, 1984; Grishin et al., 1996; Ayris and Delmelle, 2012). As a result, crop fields impacted by ash deposition produce lower- or poor-quality harvests that can translate into significant economic losses to farmers and food shortages at the local or even regional scale and even more so when subsistence agriculture dominates (Neild et al., 1998; Wilson et al., 2007; Ligot et al., 2022).

In this context, the development of strategies that can support disaster risk reduction and strengthen resilience for agrarian communities in volcanically active regions is critical, especially in less economically developed countries

(FAO, 2021). Such measures require a sound understanding of agriculture vulnerability to ashfall (UNDRO, 1980; Jenkins et al., 2015; Craig et al., 2021). Over the past 15 years, a dozen or so of post-eruption impact assessments (post-EIA) have contributed to document the responses of farming systems exposed to ash (e.g. Wilson et al., 2007, 2011; Magill et al., 2013; Blake et al., 2015; Craig et al., 2016a, b; Ligot et al., 2022). These field-based investigations have underpinned the development of empirical relationships that link ash accumulation (also referred to as ash mass load or deposit thickness) to an estimated level of production loss for different agriculture types characterised by specific vulnerabilities (Wilson and Kaye, 2007; Jenkins et al., 2014; Craig et al., 2021). In parallel, new methodologies harvesting the potential of big Earth observation data acquired from satellite-based sensors (e.g. Landsat, MODIS, and Sentinel) and interpretable machine learning are being developed to complement post-EIA studies (Biass et al., 2022).

Despite these recent efforts, current relationships between ash and crop production loss remain overshadowed by uncertainties (Jenkins et al., 2015), which are rooted in three main sources. Firstly, they lean on limited observational data, acquired in post-EIA studies. Most of these have been conducted in temperate volcanic regions, but tropical and semi-arid environments are increasingly receiving attention. Secondly, it is assumed that ground ash accumulation (thickness or ash mass load) is the principal hazard intensity metric governing the impact level on crops. However, other volcanic (e.g. ash grain size, surface composition) and non-volcanic factors (e.g. environmental conditions, plant traits, crop development stage) play a key role in dictating impact and vulnerability (Jenkins et al., 2015; Ligot et al., 2022). Finally, current approaches lack an impact metric that can be applied to assess crop yield loss from ashfall. These limitations are hindering the development of accurate process-based risk assessment models that can inform targeted strategies to build the resilience of agriculture-based communities in the case of an explosive eruption, for example in relation to aid allocation, land-use planning and insuring.

Jenkins et al. (2022) estimated that an explosive eruption of 4 on the Volcanic Explosivity Index (VEI, Newhall and Self, 1982) on the island of Java, Indonesia, has on average a 50 % probability of affecting $\sim 700\,\mathrm{km}^2$ of crops with $5\,\mathrm{kg\,m}^{-2}$ of ash. The surface area potentially affected by ash fallout is ~ 17 times larger for an eruption of VEI 5. Ash deposits thin exponentially from the source. Close to the vent, ash fallout usually results in destructive impacts, e.g. smothering of the vegetation and direct mechanical breakage of plants' parts (leaves, twigs, stem) (Ayris and Delmelle, 2012; Arnalds, 2013; Jenkins et al., 2015; Craig et al., 2021). With increasing distance from the vent, impacts gradually become less severe disturbances. Thin ash deposits, able to affect several hundred to thousands of square kilometres, retain the potential to cause serious crop yield loss without threatening plant structural integrity (Magill et al., 2013; Ligot et al., 2022). At distal sites, in the absence of structural damage to plants, the capacity of ashfall to initiate damage to crop yield hinges on the capacity of leaves coated with a thin ash deposit to operate photosynthesis and produce biomass. While the release of harmful chemical compounds from ash can cause leaf tissue injuries and affect photosynthesis, this effect, if occurring, is limited to ash emissions from phreatic and phreatomagmatic eruptions (Le Guern et al., 1980; Ayris and Delmelle, 2012). For purely magmatic explosive events, impacts on crops over a wide area far from the volcano primarily relate to the shading effect exerted by the presence of solid particles on leaf surfaces, reducing light interception and decreasing photosynthetic activity (Thompson et al., 1984; Hirano et al., 1995). Thus, ash retention on foliage (i.e. the percentage of the leaf surface area covered with ash) is a critical variable for developing accurate models that can assess and predict widespread impacts on crop production from ashfall. Although ash grain size, leaf pubescence, and ambient humidity have been suspected to affect ash retention on foliage, we are still lacking a (i) systematic investigation of factors controlling ash retention on foliage and a (ii) quantitative impact metric reflecting crop production loss.

Here, we adopt an experimental setup to investigate the influence of ash grain size, leaf pubescence, and humidity conditions at leaf surfaces on ash retention on crop foliage using tomato and chilli pepper as model plants. By integrating the effect of both volcanic and non-volcanic factors on ash retention, we formulate a novel conceptual model that uses LAI as the impact metric for predicting crop yield loss when ash deposited on plants does not threaten their integrity.

2 Material and methods

2.1 Plant material and growing conditions

Tomato (*Solanum lycopersicum* L.) and chilli pepper (*Capsicum annuum* L.) plants were chosen to illustrate contrasting behaviours between plants of agronomical interest; they have a similar stand in the early growth period, but tomato plants have hairy leaves, whereas chilli pepper plants have glabrous leaves. The experiment took place in Belgium. The seeds were sown in a sieved peat-based compost (pH 5–6.5) maintained at 24 °C. Four weeks after sowing, the seedlings were transplanted in 1 L plastic pots also filled with peat-based compost. The average day and night temperatures in the greenhouse were 30 and 24 °C, respectively. Due to summer heats in Belgium, temperature during the day occasionally rose above 35 °C. Combined with natural light, the use of LED lamps ($120\,\mu\mathrm{moles\,m}^{-2}\,\mathrm{s}^{-1}$) provided a 16 h photoperiod. Tomato and chilli pepper plants were watered three times a week. They were exposed to ash 6 weeks after sowing, when tomato and chilli pepper plants were at the seven- and eight-leaf stage, respectively. The corresponding plant heights were ~ 40 and ~ 30 cm. The foliage surface

area was ~ 400 and $\sim 100\,cm^2$ for tomato and chilli pepper plants, respectively.

2.2 Simulated ash deposition

We investigated the influence of ash grain size on the ability of tomato and chilli pepper leaves to retain ash under dry and moist conditions. Six ash size ranges were tested, namely ≤ 90, 90–125, 125–250, 250–500, 500–1000, and 1000–2000 µm. Each size range was tested in combination with either dry or wet leaf surface conditions, i.e. a total of 24 treatments for both crops. A treatment consisted of 15 replicates, corresponding to 360 measurements in total. The ash material was obtained by crushing a phonolite rock (bulk composition: $SiO_2 = 52.5\,wt\,\%$, $Al_2O_3 = 21.8\,wt\,\%$, $K_2O = 9.6\,wt\,\%$, $Na_2O = 7.8\,wt\,\%$, $Fe_2O_3 = 2.9\,wt\,\%$, $CaO = 1.5\,wt\,\%$, $TiO_2 = 0.3\,wt\,\%$, $MgO = 0.2\,wt\,\%$, density $= 2.54\,g\,cm^{-3}$; Van den Bogaard and Schmincke, 1984) obtained from a quarry close to the Laacher See volcano in Germany. The shape characteristics of the six ash size fractions obtained by grinding the Laacher See phonolite were examined by scanning electron microscopy (SEM). The SEM images (Fig. S1 in the Supplement) reveal that, regardless of their size, most particles are blocky, but rounded and platy shapes also occur. Similar shapes are commonly reported for ash particles from explosive eruptions (e.g. Wohletz, 1983; Coltelli et al., 2008; Nurfiani and Bouvet de Maisonneuve, 2017). However, the vesicular ash type that is also often associated with the magma fragmentation of gas-rich magmas cannot be generated by rock grinding and was absent in our experimental ash material. The crushed phonolite was dry sieved for 10 min using an AS 200 Control Retsh vibrating sieve shaker with six sieves (90, 125, 250, 500, 1000, 2000 µm). The five size fractions coarser than 90 µm were wet sieved to remove particles < 90 µm. The grain size distribution of the six ash size ranges was measured between 0.04 and 2000 µm by laser diffraction (Beckman Coulter LS13 320) (Fig. S2). The median diameter was equal to 5, 98, 174, 401, 774, and 1465 µm for the ≤ 90, 90–125, 125–250, 250–500, 500–1000, and 1000–2000 µm ash size ranges, respectively.

An ash load of $\sim 570\,g\,m^{-2}$ was selected for the experiments. Assuming a bulk density of $1\,g\,cm^{-3}$ for the ash deposit (Eychenne et al., 2012), this corresponds to a relatively thin deposit of ~ 0.6 mm (i.e. considering a bulk deposit density of $1\,g\,cm^{-3}$; Eychenne et al., 2012), best representing accumulations encountered at distal sites (and over wide areas) affected by ash fallout from explosive eruptions (Fierstein and Nathenson, 1992; Jenkins et al., 2022). Pre-tests carried out with higher ash loads ($\geq 1000\,g\,m^{-2}$) already led to lodging of some tomato and chilli pepper plant specimens, a phenomenon that needed to be avoided in order to maximise the experiment's reproducibility. Neild et al. (1998) and Craig (2015) consider that an ash mass load of 6–30 $kg\,m^{-2}$ on plants leads to mechanical damage. Our observations indicate that lower loads can affect crop plants. In other words, the threshold value above which mechanical injury occurs varies with plant phenotype (i.e. the combination of plant genotype and environment).

The selected ash load was applied uniformly to each plant using a homemade ashfall simulator (Fig. S3). The device consists of a 135 cm high PVC tube (with a diameter of 29.5 cm) with three 1 mm opening meshes placed 75, 110, and 120 cm from the tube base. The ash fractions < 1000 µm were poured carefully through a 2 cm mesh sieve installed on the top of the PVC tube. The bouncing of the ash particles passing through the three inner 1 cm sieves allowed the formation of a uniform deposit. The application of the coarsest ash (1000–2000 µm) was carried out with the same device, but the inner meshes were removed. Wet conditions at leaf surfaces were obtained by spreading ~ 1.5 g of water on each plant using a commercial manual sprayer held 1 m above the ground. In order to simulate the presence of water droplets on plant leaves, we applied four sprays of water, one in each cardinal direction just before ash treatment. Water spraying of the plant foliage, ash application, and photo acquisition all took place within the black chamber. Less than 5 min elapsed between the spraying operation and photo acquisition of the ash-treated plant (Fig. S4).

2.3 Estimating the foliar cover from digital photos

We took photos of each plant before and immediately after ash treatment (Fig. S4). To minimise uncontrolled variations in light colour and brightness, plants were photographed in a $1.6\,m \times 1.2\,m \times 2.2\,m$ black chamber equipped with four LED bulbs (6.5 W, cold white, Figs. S3 and S4). We used a DX Nikon camera with an AF-S DX NIKKOR 18–55 mm f/3.5–5.6G VR II lens mounted on a 0.9 m high tripod. Sheets of paper were placed on the floor and plant pot to produce a uniform background. A ribbon placed in a fixed position provided a reference scale.

We analysed the digital photos taken just before and after ash application with ImageJ 1.52 (Schindelin et al., 2015). The foliar cover, a measure of the vertical projection of exposed leaf area, was estimated using a dedicated macro (https://github.com/NoaLigot/ImageJ-macro.git, last access: 29 March 2023). While digital photos are recorded as a raster of red–green–blue (RGB) pixels, the values are not standardised and can vary depending on the camera (Darge et al., 2019). The ImageJ macro transforms the RGB colour space into the International Commission on Illumination (CIE) 1976 L*a*b* colour space (McLaren, 1976), which has linear measures of lightness (L*) and two colour dimensions (a* and b*). The a* dimension represents a spectrum from green (negative) to magenta (positive), and the b* dimension represents a spectrum from blue (negative) to yellow (positive). The a* attribute is useful to identify green pixels and was used in the ImageJ macro to identify and select green parts of leaves. Values of 1 and 0 are attributed to a green

and non-green (background) pixel, respectively. This allows for delineation of the shape of the green leaf portion and calculation of its surface area.

2.4 Data treatment

The percentage of foliar cover coated with ash was inferred for each plant by comparing the foliar cover estimated from the image analysis, before and after ash application. A Tukey honest significant difference (HSD) test was applied to determine if means differ between treatments. Tomato and chilli pepper plant measurements carried out under dry and wet leaf surface conditions were processed separately; i.e. four sub-datasets were used in order to compare the means separately for each combination of crop and moisture conditions.

3 Results

3.1 Foliar cover coated with ash

The percentage of foliar cover coated with ash ranged from 0 % to 99 %, with an average value of 36 ± 33 % (Table S1 in the Supplement). The effect of ash grain size, humidity conditions at leaf surfaces, and leaf pubescence on the foliar cover coated with ash is illustrated in Fig. 1. In general, foliar cover coated with ash increased with decreasing ash grain size. Grain size ≥ 500 µm covered only 10 % of the foliar cover, with coverage increasing up to ~ 90 % for ash ≤ 90 µm. Wetting of tomato and chilli pepper leaves prior to ash application had no significant effect on the retention of fine ash (≤ 90 µm). Nevertheless, significant higher tomato and chilli pepper leaf surface coverages ($+17 \pm 5$ % and $+31 \pm 10$ %) were inferred for intermediate ash grain sizes between 90 and 500 µm (Tables S1 and S2). We also note that for the ash grain size ranges 125–250 and 250–500 µm in dry conditions, coverage of tomato leaves with ash was significantly greater, by ~ 30 % and 20 % on average, compared to chilli pepper leaves.

3.2 Quantifying ash retention as a function of grain size

Using the experimental results obtained for tomato and chilli pepper plants (Fig. 1), we predicted the percentage of foliar cover coated with ash as a function of grain size when leaf surfaces are dry or wet. Five convex models (i.e. exponential decay, power curve, rectangular hyperbola, asymptotic curve, and logarithmic curve) were fitted to the data points using the aomisc and nlme packages in R (Onofri, 2020; Pinheiro and Bates, 2022) (Fig. S5). The median grain size was used to represent the corresponding grain size range. A lack-of-fit sum of squares test was applied to evaluate the relevance of each model. Since the five models have different numbers of parameters, their test statistics (F^*) could not be compared directly. Instead, the models were assessed based on their p values (Table S3). All the models have p values > 5 %, with no evident lack of fit. The exponential decay model had the highest p value for the four sub-datasets (0.82, 0.98, 1, and 1 for dry tomato, wet tomato, dry chilli pepper, and wet chilli pepper, respectively), and it was chosen for the predictions.

Quantile regressions using the exponential decay model indicate that for 500 µm ash particles, there is a 50 % chance to cover ~ 10 % and ~ 27 % of tomato foliar cover in dry and wet conditions, respectively (Fig. 2). Similarly, for chilli pepper, foliar covers of < 1 % and 20 % are estimated in dry and wet conditions, respectively. By the same tenet, there is a 50 % probability that ash with a median of 63 µm in diameter covers up to ~ 67 % (dry conditions) and ~ 77 % (wet conditions) of the foliar cover in tomato and ~ 51 % (dry conditions) and ~ 78 % (wet conditions) of the foliar cover in chilli pepper.

3.3 Distribution of ash retention on the foliar cover

In addition to controlling ash retention on leaves, grain size, conditions of humidity at leaf surfaces, and leaf pubescence affect the location of ash retention (Fig. 3). For tomato plants in dry conditions, ash ≤ 90 µm tended to be lodged on the leaf surface wherever it had settled. For glabrous chilli pepper leaves, leaf angle dictates if the ash particles remain on the leaf surface after deposition or slide off and relocate elsewhere. Ash with intermediate grain sizes between 90 and 500 µm behaved differently, depending on humidity conditions. For both tomato and chilli pepper plants, the ash material was found mainly along the primary and secondary veins of the horizontal upper leaves when they were dry. However, in wet conditions, ash was more homogeneously distributed over the leaf surface. Coarser ash (≥ 500 µm) accumulated preferentially in the folds of growing leaves.

4 Discussion

4.1 Influence of grain size on ash retention

The foliar cover coated with ash increases exponentially (from ~ 10 % to 90 %) when grain size decreases (from 500 to 90 µm), whether in dry or humid leaf conditions (Fig. 2). This relationship was established for a single ash mass load ($\sim 570\,\mathrm{g\,m^{-2}}$). For ash in the intermediate size range, a higher load could result in enhanced retention of the particles, particularly along the primary and secondary leaf veins, as these consist of less elastic tissues that can better absorb the kinetic energy of impinging ash particles of intermediate grain size. However, for fine ash, we do not expect more retention to occur if tomato and chilli pepper leaves were exposed to higher loads because a large proportion of the uncovered foliage is comprised of leaves that, due to their steep angle, cannot retain ash particles efficiently. As mentioned earlier, coarse ash particles tend to lodge primarily on leaf folds. Thus, their retention on foliage will likely be

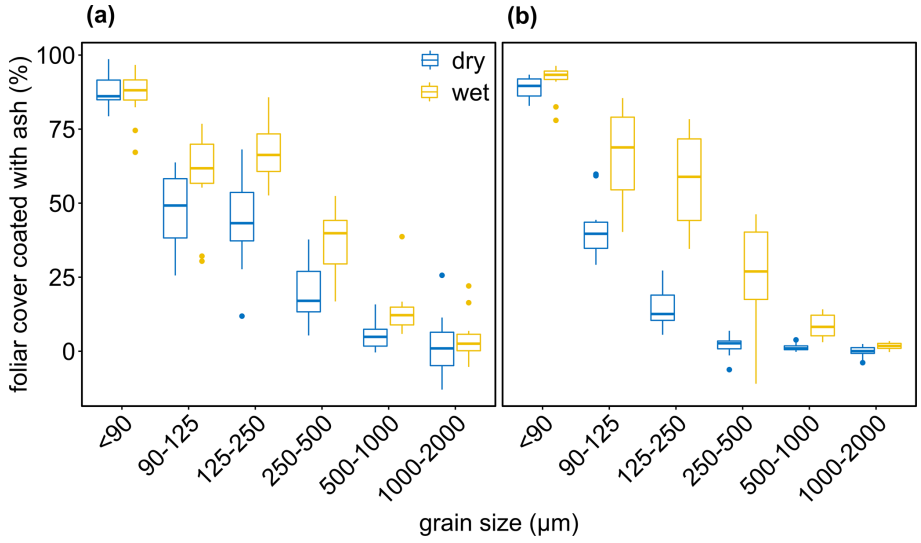

Figure 1. Percentage of foliar cover coated with ash for tomato plants, i.e. which have pubescent leaves, **(a)** and chilli pepper plants, which have glabrous leaves **(b)**. The percentage of foliage cover was measured for the six grain size ranges tested in dry and wet conditions at leaf surfaces. Each boxplot represents 15 repetitions. The median value sits within the box and represents the centre of the data. A total of 50 % of the data values lies above the median, and 50 % lies below the median. Measurement outliers are displayed as dots.

limited by the number of leaf folds. Overall, we anticipate that for ash load values $> 570\,\mathrm{g\,m^{-2}}$, the exponential dependence of ash retention on ash grain size will start to degrade, and instead a linear relationship would be a better model. The increased ash retention when grain size decreases is in accordance with the field observations of Miller (1967) after the 1963 eruption of Irazú volcano, Costa Rica, who found a higher degree of retention of the smaller particles by crop foliage (alfalfa, corn, bean, beet, cabbage, carrot, pea, pepper, potato, radish, and squash). Johnson and Lovaas (1969) and Witherspoon and Taylor (1970) reached a similar conclusion after dusting various crops (alfalfa, corn, squash, soybean, sorghum, peanut, and clover) with quartz powders differing in grain size (88–175 and 175–350, as well as 44–88 and 88–175 µm).

The fate of a solid particle falling from the atmosphere and hitting a leaf surface will depend on how much of its initial kinetic energy is absorbed through tissue deformation (Vogel, 1989; Niklas, 1999; Benson, 2015). Ignoring aggregation processes and considering a constant particle bulk density, the coarser the particles, the larger their terminal fall velocity and thus kinetic energy (Dellino et al., 2005; Benson, 2015). If particles retain enough kinetic energy after impact, they can bounce back and be ejected off the leaf or deposited elsewhere (Gregory, 1961; Chamberlain, 1967; Starr, 1967; Chamberlain and Chadwick, 1972). Otherwise, they will settle on the upper side of leaves, although they may be subsequently displaced as new particles impinge on the leaf surface. Based on the drag model for non-spherical particles of Bagheri and Bonadonna (2016), we estimated the terminal fall velocity of individual particles of 10, 100, 170, 410, 710, and 1470 µm, representing the median values of the six ash size ranges used in our experiment. Terminal fall velocity increases with grain size and is 5 times lower for particles of 100 µm diameter (assimilated to the fine-ash fraction) than for particles of 410 µm diameter (corresponding to coarse ash) (Table S4). This result suggests that the kinetic energy of the finest ash particles is $\sim 10\,000$ times smaller than that of the coarsest material. The low kinetic energy of fine particles probably explains why ash in the ≤ 90 µm size fraction produces a greater foliar cover compared to ash ≥ 500 µm (Fig. 2). In contrast, coarse ash particles with higher kinetic energy will tend to lodge on less elastic leaf structures, such as primary and secondary veins and folds (Fig. 3). As mentioned above (Sect. 2), an inherent limitation of our experimental study is that the ash material did not contain the vesicular particles that are usually found in various proportions of ash fallout from explosive eruptions. We speculate that the irregular shape of vesicular ash could enhance retention on foliage, perhaps even more so if the leaf surfaces are pubescent or wet. Thus, our measurements may be regarded as conservative estimates.

4.2 Influence of leaf pubescence on ash retention

On average, ash particles in the intermediate size range 125–500 µm cover ~ 25 % more foliar cover in tomato plants than in chilli pepper plants (Fig. 2 and Table S1). This is attributed primarily to the presence of leaf hairs in tomato plants. Sæbø et al. (2012) and Ram et al. (2012) demonstrated that dust accumulation on the foliage of various trees and shrubs is proportional to leaf hair density. Leaf hairs enhance the dust collection area and capacity to absorb the falling particles'

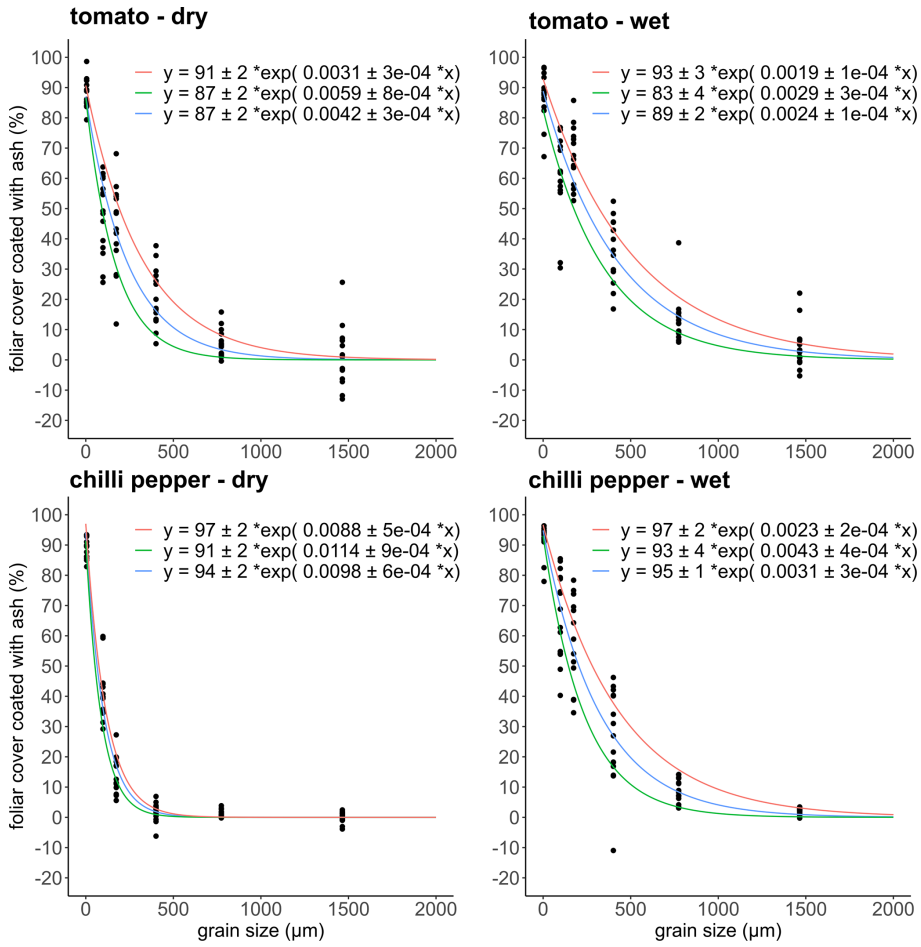

Figure 2. Quantile regression with the first quartile (green), median (blue), and third quartile (red) for tomato and chilli pepper plants in dry and wet conditions at leaf surfaces.

kinetic energy. In addition, leaf pubescence may prevent particles from sliding off the leaf surface. By increasing friction on particles, leaf hairs counteract the gravity force generated by mass loading on the leaf surface which pulls a leaf downward (Smith and Staskawicz, 1977). In our experiments, ash $\leq 90\,\mu m$ adhered to the tip of pubescent leaves with a steep inclination angle in tomato plants, whereas it barely encroached on the glabrous surface of chilli pepper leaves (Fig. 3). Previous field observations of ash-impacted crops have also highlighted a stronger adherence of ash on pubescent leaves (such as barley, corn, tobacco, tomato, and apple tree) and hairy fruits (such as peach, apricot, kiwi, strawberry, and raspberry) (Miller, 1967; Cook et al., 1981; Wilson et al., 2007; Sword-Daniels et al., 2011; Ligot et al., 2022). Witherspoon and Taylor (1970) concluded that the pubescent leaves of squash and soybean favour a uniform retention of quartz particles (88–175 µm). In contrast, the glabrous leaves of rose plants exposed to the 1963 eruption of Irazú volcano, Costa Rica, collected little ash material (Miller, 1967).

4.3 Influence of humidity conditions at leaf surfaces on ash retention

Wetting of leaves prior to application of ash with an intermediate grain size of 90–500 µm increased the foliar cover coated with ash of tomato and chilli pepper plants by $17 \pm 5\,\%$ and $31 \pm 10\,\%$, respectively (Fig. 2 and Table S2). We also noted that the ash deposit that formed on pre-wetted leaves appeared more homogeneous compared to that observed when the leaf surface was dry (Fig. 3). Similarly, Miller (1967) reported during the 1963 eruption of Irazú that wet leaf surfaces facilitated retention of ash $< 300\,\mu m$ and formation of a homogeneous deposit. Enhanced ash retention on wet leaves likely relates to the surface tension generated by water molecules present on the leaf surface (Tabor, 1977; Israelachvili, 2011). Conversely, as plant leaves are hydrophobic (Bhushan and Jung, 2006), more water on leaves, such as after a heavy or prolonged light rain, could lead to the formation of large water droplets that are able to erode particles from the leaf surface, thereby reducing ash retention.

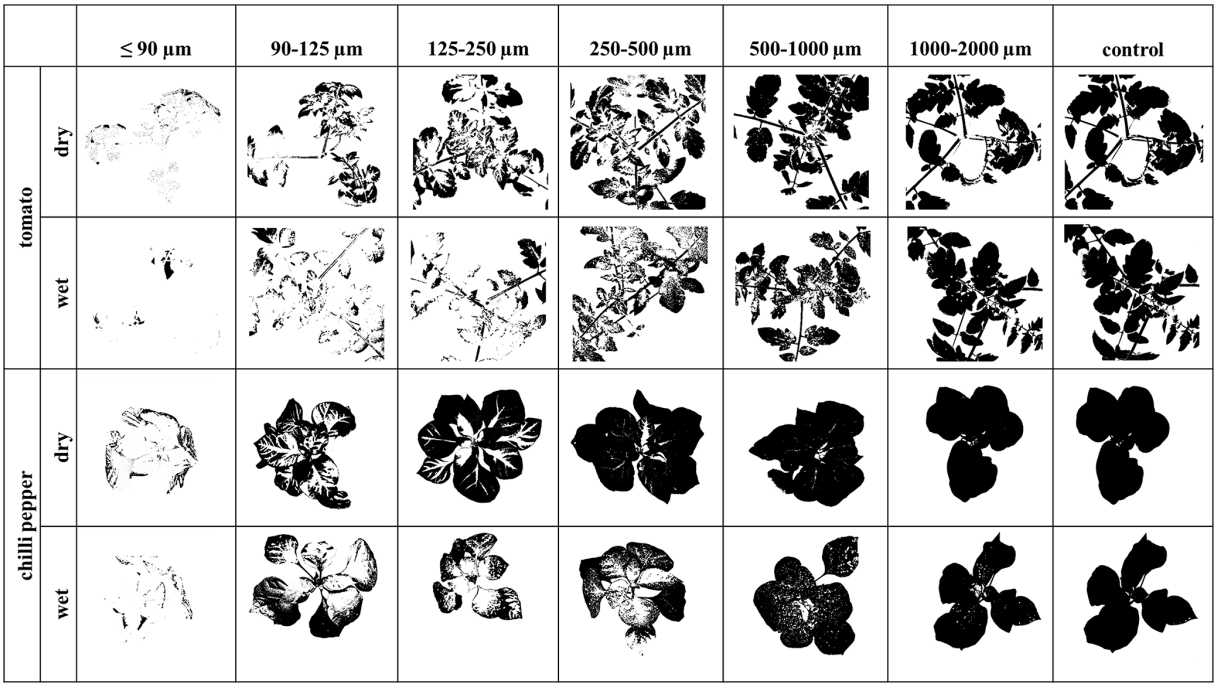

Figure 3. Photos processed with ImageJ of tomato and chilli pepper plants before (control) and after exposure to $\sim 570\,\mathrm{g\,m^{-2}}$ of ash varying in grain size (≤ 90, 90–125, 125–250, 250–500, 500–1000, 1000–2000 µm) and in dry and wet conditions at leaf surfaces. The part of the foliar cover depicted in black corresponds to the green leaf surface area that was not covered with ash. The image surface area is equivalent to $\sim 800\,\mathrm{cm^2}$. The original photos of the ash-covered plants are provided in the Supplement (Fig. S6).

4.4 Modelling potential yield loss in tomato and chilli pepper plants exposed to ash

Our experimental results indicate that $\sim 570\,\mathrm{g\,m^{-2}}$ fine ash can readily cover the upper side of leaves (Fig. 2). Assuming an ash material comprised of spherical particles 90 µm in diameter and with a density of $2.54\,\mathrm{g\,cm^{-3}}$ (i.e. the density of phonolite), we calculated that a mass load as low as $\sim 8.6\,\mathrm{g\,m^{-2}}$ can form a monolayer deposit on a leaf surface. While this estimate represents an oversimplified situation, it is more than 50 times less than the ash load ($\sim 570\,\mathrm{g\,m^{-2}}$) used in our experiment. Since fine particles are ubiquitous – albeit in various proportions – in ash fallout (Rust and Cashman, 2011; Costa et al., 2016), an ash coating on leaf surfaces is likely to be the rule in vegetated areas affected by explosive eruptions. Importantly, the presence of solid particles on foliage exerts a shading effect, which reduces light interception (LI, dimensionless) by leaves (Thompson et al., 1984; Hirano et al., 1990). For example, Hirano et al. (1991) measured a $\sim 20\,\%$ decrease in LI after treating mandarin tree leaves with only $4\,\mathrm{g\,m^{-2}}$ of road dust (0.1–100 µm). Similarly, the deposition of $10\,\mathrm{g\,m^{-2}}$ of ash (0–100 µm) on cucumber plants led to a $\sim 20\,\%$ reduction in LI (Hirano et al., 1992).

Considering that LI drives the net photosynthesis rate, and thereby total biomass production (Wilson, 1967; Biscoe et al., 1977; Monteith, 1977; Weraduwage et al., 2015), we contend that even a thin ash deposit on crop leaves can drive yield loss. Thus, the interference of ash with LI provides an indirect mean to predict the potential crop production loss for ash mass loads below the threshold ($\sim$ 6–30 $\mathrm{kg\,m^{-2}}$ mass load) of direct mechanical damage to plants. Although we did not measure LI in our experiment, this parameter can be inferred using the following expression (Monteith, 1969):

$$\mathrm{LI} = \left(1 - e^{-k \times \mathrm{LAI}}\right), \quad (1)$$

where k is the light interception coefficient (dimensionless). The temporal evolution of LAI during plant growth has been documented for tomato and chilli pepper plants in several studies (e.g. Campillo et al., 2010; Monte et al., 2013; Al Mamun Hossain et al., 2017; Mendoza Perez et al., 2017), allowing for the estimate of LI via Eq. (1).

In light-limited situations, i.e. the other growth parameters (e.g. water and nutrient status) being optimum, the daily biomass accumulation by crop canopy ($\mathrm{CBIO_c}$, $\mathrm{g\,m^{-2}\,d^{-1}}$) depends on LI according to (Monteith, 1972; Hatfield, 2014)

$$\mathrm{CBIO_c} = Q \times \mathrm{LI} \times \mathrm{RUE}, \quad (2)$$

where Q is the incident radiation ($\mathrm{MJ\,m^{-2}\,d^{-1}}$) and RUE ($\mathrm{g\,MJ^{-1}}$) the radiation use efficiency. Representative values for Q in Belgium ($10.6\,\mathrm{MJ\,m^{-2}\,d^{-1}}$, warm temperate humid climate, Solargis, 2022) and RUE are available from the scientific literature (Table S5). The crop-harvested biomass

($CBIO_h$, $g\,m^{-2}\,d^{-1}$) is calculated as the sum of the $CBIO_c$ in the time period considered (i.e. number of days elapsed between transplanting and harvest) multiplied with the harvest index, i.e. the fraction of the total aboveground biomass allocated to the harvested parts of the plant (HI, dimensionless) (Kemanian et al., 2007; Hay, 2008):

$$CBIO_h = \sum_{sowing}^{harvest} CBIO_c \times HI. \quad (3)$$

Figure 4 depicts the concepts underpinning Eqs. (1), (2), and (3).

We consider two effects of ash on plant yield: reduction in LAI and premature biomass senescence. The former leads to lower accumulated biomass after the formation of the ash deposit, whereas the latter is responsible for a loss of biomass that accumulated prior to ashfall. We hypothesise that LAI reduction and biomass dying of crop plants exposed to ash are directly proportional to the percentage of foliar cover coated with ash deposits (Fig. 2), presupposing that ash-affected leaves lose their ability to perform photosynthesis efficiently. Based on this, and using Eqs. (1), (2), and (3), potential crop yield loss ($CYL_{\%}$, %) can be deduced by comparing the harvested biomass in the absence ($CBIO_h^{no\ ash}$) and presence ($CBIO_h^{ash}$) of ash (see Supplement):

$$CYL_{\%} = 100 \times \frac{CBIO_h^{no\ ash} - CBIO_h^{ash}}{CBIO_h^{no\ ash}}. \quad (4)$$

To illustrate our approach, we estimated $CYL_{\%}$ for tomato and chilli pepper plants exposed to ~ 0.6 mm ($\sim 570\,g\,m^{-2}$) of ash. We tested different ash size distributions and evaluated the influence of humidity conditions at leaf surfaces on ash retention. Two scenarios of plant exposure to ashfall were considered: one in which 25 % of the plant growth period is completed (i.e. 32 d after transplanting for tomato plants and 57 d after transplanting for chilli pepper plants) and one in which 75 % is achieved (i.e. 97 d after transplanting for tomato plants and 172 d after transplanting for chilli pepper plants). The daily LAI evolution of tomato and chilli pepper plants during growth was computed in R using published data (see Table S5 in the Supplement).

In our model, the entire plant canopy received the same amount of ash, although some leaves may have been less exposed due to their position on the stem. As the ash mass load is low ($570\,g\,m^{-2}$), we also considered that ash deposition on leaves neither halt plant growth nor production of new leaves (Neild et al., 1998; Ligot, 2022). On the day of the eruption, the LAI is reduced by an amount corresponding to the percentage of foliar cover coated with ash. On the following days, it re-increases as new leaf formation resumes at a rate similar to that before exposure to ash. If time permits, the LAI may reach a value identical to that of a plant that would not have received ash. The calculated temporal evolution of the LAI of a tomato plant that has completed 25 % of its growth period when it receives ash (90–125 µm in diameter, mass load of $\sim 570\,g\,m^{-2}$) in dry conditions is illustrated in Fig. 5a. A similar temporal evolution of LAI is obtained for a chilli pepper plant (Fig. S7).

The presence of ash on plant canopy may lead to premature leaf senescence (as reported by Miller, 1967; Neild et al., 1998; Wilson et al., 2007; Ligot et al., 2022), impacting $CBIO_h$ (Eq. 3). To account for this effect, we subtracted the ash-coated leaf biomass from the total canopy biomass, the latter being comprised of the leaves and stem. For tomato and chilli pepper plants, leaf biomass represents ~ 60 % of canopy biomass (Kleinhenz et al., 2006; Elia and Conversa, 2012; Poorter et al., 2015). The leaf biomass fraction affected by ash can be inferred from Fig. 1. Resolving Eqs. (1) and (2), the temporal evolution of $CBIO_c$ for tomato or chilli pepper plants subjected to ash can be predicted. Figure 5b illustrates this for tomato plants exposed in dry conditions to ash deposition (90–125 µm in diameter; mass load of $\sim 570\,g\,m^{-2}$) 32 d after transplanting (i.e. at 25 % of growth period). Since the leaf-to-canopy biomass ratio and the percentage of leaf biomass covered with ash which dies are equal for both crops (Table S5, Kleinhenz et al., 2006; Elia and Conversa, 2012; Poorter et al., 2015), a similar trend is inferred for chilli pepper plants (Fig. S7).

As detailed above, ash impact on $CBIO_h$ is modulated by different factors, including the LAI fraction that becomes photosynthetically inactive due to the presence of ash coatings on leaves (i), number of days elapsed between the ash deposition and emergence of new leaves (ii), leaf-to-canopy biomass ratio (iii), and percentage of leaf biomass covered with ash which eventually dies (iv). Our model calculations revealed that the crop growth period determines the relative importance of each of these factors in determining $CYL_{\%}$. For example, if 90 µm ash affects tomato and chilli pepper plants in dry conditions at 25 % of their growth period, $CYL_{\%}$ is the most sensitive to (i) and (ii), whereas for older plants that have completed 75 % of their growth, (iii) and (iv) are the main factors driving $CYL_{\%}$ (see Supplement).

In order to assess the error on $CYL_{\%}$ estimates, we applied a stochastic approach with 10 000 simulation runs using a random value for each of the four factors (as listed above) that can influence the final model output. We posited that the values taken by factors (iii) and (iv) follow a Gaussian distribution (Table S5), whereas variable (i) and (ii), which are always in the range 0–1 and positive, respectively, are described by a truncated Gaussian distribution. Figure 6 shows the uncertainties on $CYL_{\%}$ as computed by fitting the first and third quartiles around the median $CYL_{\%}$ value for tomato and chilli pepper plants exposed to ash of different grain sizes, either in dry or wet leaf conditions. Calculations were repeated for plants that receive ash when at 25 % and 75 % of their growth period. For tomato plants, $CYL_{\%}$ increases with decreasing ash grain size (Fig. 6). Tomato plants at 25 % of their growth may experience a 2 %–17 % decrease in yield, depending on grain size and humidity conditions at leaf surfaces. A significantly higher $CYL_{\%}$ (0 %–42 %) is anticipated when ash affects plants at 75 % of their growth. A

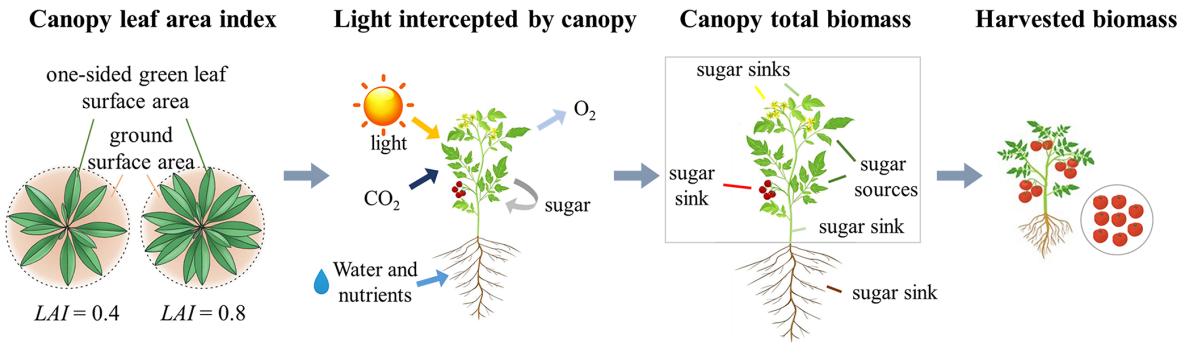

Figure 4. Illustration conceptualising the relationships between the canopy leaf area index (LAI), light interception by canopy, canopy total biomass, and harvested biomass.

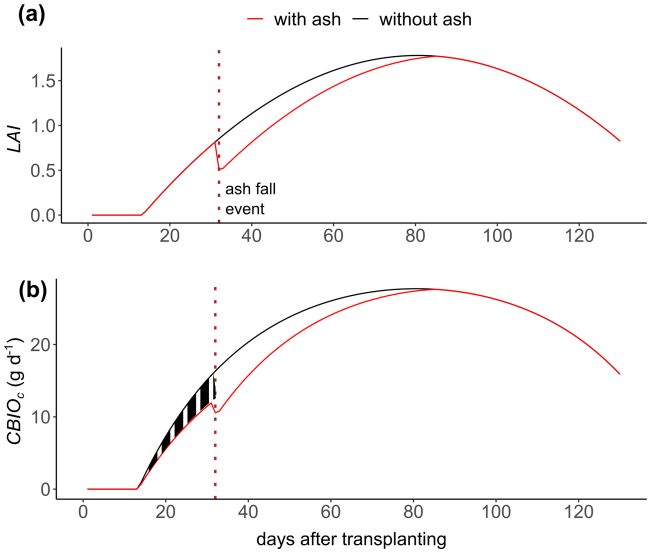

Figure 5. Temporal evolution of leaf area index (LAI) **(a)** and daily biomass accumulation ($CBIO_c$) **(b)** of a tomato plant exposed to $\sim 570\,g\,m^{-2}$ of ash (size range: 90–125 µm) 32 d after transplanting (i.e. at 25 % of the growth period) in dry leaf surface conditions. The hatched area represents the leaf biomass produced by the plant before the ashfall event and which will undergo premature senescence after it. The ash-covered leaf biomass is inferred from the leaf-to-canopy biomass ratio (i.e. 60 %) and the percentage of leaf biomass covered with ash (i.e. 48 % for tomato plants in dry leaf surface conditions, Table S1).

similar pattern emerges for chilli pepper plants where $CYL_{\%}$ varies between 1 %–17 % and 0 %–46 % when considering that the plant receives ash when at 25 % and 75 % of its growth period, respectively (Fig. 6). For intermediate ash grain sizes between 125 and 500 µm, the $CYL_{\%}$ is 5 %, 3 %, 8 %, and 4 % greater for tomato plants compared to chilli pepper plants when exposure to ash occurs at 25 % of the growth in dry conditions, 25 % of the growth in wet conditions, 75 % of the growth in dry conditions, and 75 % of the growth in wet conditions, respectively.

4.5 Towards using LAI as an impact metric for predicting potential yield loss in ash-affected crops

While the deployment of field-based post-EIA will continue to enrich our understanding of relationships between ash and crop production loss, progress is contingent on the eruption occurrence, site accessibility, limited field time, variations in environmental conditions, and incomplete ranges of ash characteristics such as thickness and grain size (Jenkins et al., 2015). Here, we have shown, using established theories of plant–physiological processes (Monteith, 1969, 1972), how empirical data from experimental testing can be transformed into quantitative insights for predicting potential yield loss in tomato and chilli pepper crops exposed to ash. Changes in LAI and premature biomass loss in ash-affected crops are interpreted as dependent on ash retention on leaves, a process influenced by grain size, plant traits, and environmental conditions (Fig. 1). Here, we exclude the possible effect of ash surface composition on ash retention. As detailed in Eqs. (1), (2), and (3), crop yield depends on LAI, and therefore the latter is regarded as an integrative impact metric. From this, we propose that LAI measurements in crop plants subjected to ashfall offer a new method for analysing crop vulnerability and assessing potential yield loss for ash mass loads below the threshold ($\sim$ 6–30 $kg\,m^{-2}$) of direct mechanical damage to plants. The rapidly increasing ability to monitor crop characteristics, including type, LAI, and biomass, using optical and radar earth observation data (Hosseini et al., 2015; Fang et al., 2019; Rosso et al., 2022) provides an unprecedented opportunity to collect spatially and time-resolved information that can support the development of more realistic and more complete relationships between ash and crop production loss.

In order to unlock the full potential of LAI estimates for investigating the vulnerability of crops to ash events, more knowledge on how ash coatings on leaves interfere with LI is required. In our model of potential yield loss in tomato and chilli pepper plants (Fig. 6), we equated LAI reduction with the foliar cover percentage covered with ash. In essence, this means that an ash deposit on leaves renders light intercep-

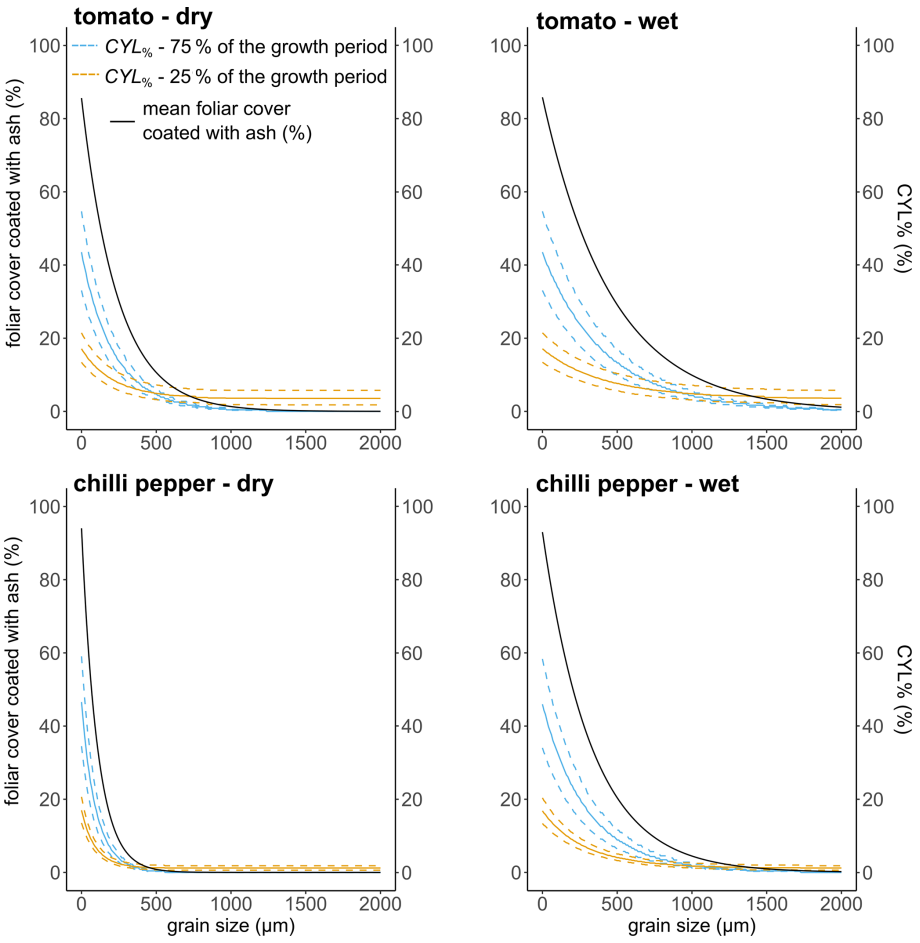

Figure 6. Potential crop yield loss ($CYL_{\%}$, first quartile, median, and third quartile) estimated for tomato and chilli pepper plants as a function of the ash grain size in dry and wet conditions at leaf surfaces.

tion inoperative. This may not always be the case because LI by a crop canopy is determined not only by the LAI of the species but also by the light absorption characteristics of the leaves (Liang et al., 2012), here modified by the ash deposit. Further laboratory investigations can generate the empirical observations needed to better constrain the changes in LI in relation to the characteristics (thickness/mass load, grain size, albedo) of the ash material deposited onto the leaf surface.

The evolution of LAI following an ash deposition event (Fig. 5a) was modelled by assuming that ash-affected plants will grow new leaves after a set period of time. Our analysis showed that $CYL_{\%}$ is sensitive to this parameter, therefore requiring adjustment depending on crop type (Klepper et al., 1982). We also note that many crops (including major ones such as wheat and corn; Hay and Porter, 2006) have a determinate growth habit and as such may not be able to sprout new leaves if they receive ash late in their development cycle. Another assumption made to evaluate the LAI trend over time is that the entire plant canopy received the same amount of ash. Although this was verified for tomato and chilli pepper plants when at the seven- and eight-leaf stage, respectively, it may not necessarily be the case at a later stage of their growth if upper leaves partly shield the surfaces of leaves located below them from direct exposure to ash. Thus, the effect of ashfall on crop LAI hinges both on plant growth characteristics and the timing of the volcanic eruption. We considered in our model that an ash deposit induces premature leaf senescence, in agreement with field observations (Miller, 1967; Neild et al., 1998; Wilson et al., 2007; Ligot et al., 2022). While this process probably relates to leaf chlorosis due to LI reduction (Bilderback, 1987; Mack, 1981; Ligot et al., 2022), its temporality and precise mechanism remain unclear. New experimental investigations with various crop plants will help to better constrain the proportion of leaf biomass affected by ash, which will be subjected to premature senescence.

We have highlighted that grain size, leaf pubescence, and humidity conditions at leaf surfaces control ash retention, which in turn drives LAI reduction. Other factors may influence ash retention. For example, leaf microstructural features such as stomatal density and the presence of a waxy epicu-

ticle have been shown to influence retention of non-volcanic dust particles (Sæbø et al., 2012; Zhang et al., 2017). In addition, in the natural environment, wind- and rain-driven erosion processes can remove ash deposited on foliage. Conversely, light rain may induce crusting of ash, prolonging its residence time on leaves (Miller, 1966; Ayris and Delmelle, 2012; Le Pennec et al., 2012; Ligot et al., 2022). The significance of these environmental variables in controlling ash retention time on leaves has never been assessed quantitatively, calling for further field and experimental investigations linking ash residence time on plants and impacts.

Finally, our approach for modelling production loss in tomato and chilli pepper crops exposed to ash neglects the impact on flowers or harvested plant parts and assumes that light interception is the main variable governing plant growth. While this is true in our study where water and nutrient supply were never limited, more stringent conditions may be encountered in crop fields subjected to ashfall. For example, an ash layer on the ground may alter water and gas movements into and through the soil and surface runoff (Ayris and Delmelle, 2012; Neslon, 2013; Tarasenko, 2018), in turn impacting the soil water balance. A better comprehension of the side effects of ash deposition on the soil plant system is needed in order to identify the primary mechanisms driving the short- and long-term consequences for crop production.

5 Conclusions

Our study highlights the usefulness of conducting experimental measurements to supplement observations obtained from post-EIA. It provides a new perspective into the volcanic and non-volcanic factors that control ash impact on crops. The experimental results obtained for tomato and chilli pepper plants demonstrate that ash retention on leaf surfaces increases with decreasing grain size and is enhanced when leaves are pubescent and wet. We also showed that, for a given ash mass load ($\sim 570\,\mathrm{g\,m^{-2}}$), the leaf surface percentage covered with ash is an exponential decay function of grain size of which the parameters are influenced by leaf pubescence and humidity conditions at leaf surfaces. Thus, we conclude that the proportion of fine material in ash fallout is an important hazard metric for assessing risk to crops. The corollary to this finding is that relying on ash thickness (or mass load) alone to anticipate crop damage from ash is inaccurate and possibly misleading.

Using the empirical relationship linking ash retention to ash grain size and equating ash retention with LAI reduction, we have developed a novel model framework to predict $\mathrm{CYL}_{\%}$. This approach identifies LAI as a promising impact metric that can be quantified for assessing crop production following an ashfall event. LAI is commonly retrieved via remote sensing measurements. The rapid deployment of new satellites allows data collection at increasingly high spatial and temporal resolution (for example, the European Space Agency's Sentinel-2 mission), paving the way for estimating LAI at the crop-field scale. Additionally, the technology gives access to FPAR (fraction of photosynthetically active radiation), i.e. the fraction of the solar radiation absorbed by live leaves for the photosynthesis activity, which should also record a reduction in light interception for leaves covered with ash. We anticipate that tapping into satellite-derived measurements will considerably improve our quantitative understanding of crop vulnerability to ash fallout. However, for exploiting their full potential, field- and laboratory-based validations are required, including experiments aimed at constraining LI/LAI reduction in relation to ash retention and characteristics. Acquiring this knowledge will significantly enhance our capacity to estimate ash-related risks to crops accurately. Governments and payout agencies need such assessments in order to develop and implement effective risk reduction strategies for ashfall damage to crops in volcanically active agricultural regions.

Code availability. The ImageJ macro to analyse the plant photos and to estimate the foliar cover coated with ash, as well as the R script to compute the daily tomato and chilli pepper plant LAI, LI, $\mathrm{CBIO_c}$, and $\mathrm{CYL}_{\%}$ are available on GitHub (https://github.com/NoaLigot/R-scipt-LAI-LI-biomass-yield-loss/blob/main/script, last access: 29 March 2023; https://doi.org/10.5281/zenodo.7781693, Ligot, 2023a; and https://github.com/NoaLigot/ImageJ-macro.git, last access: 29 March 2023; https://doi.org/10.5281/zenodo.7781728, Ligot, 2023b, respectively).

Data availability. All raw data can be provided by the corresponding author upon request.

Supplement. The supplement related to this article is available online at: https://doi.org/10.5194/nhess-23-1355-2023-supplement.

Author contributions. NL, PD, and GL conceptualised the experiments, and NL carried them out. PB advised on the statistical analysis and modelling approach. NL analysed the data, wrote the R script, and ran the simulations with the help of SB. NL and PD wrote the original draft with contributions from all co-authors. PD secured funding for this research and provided the resources.

Competing interests. The contact author has declared that none of the authors has any competing interests.

Disclaimer. Publisher's note: Copernicus Publications remains neutral with regard to jurisdictional claims in published maps and institutional affiliations.

Acknowledgements. Noa Ligot's doctoral research is supported by the Fonds National de la Recherche Scientifique (FSR-FNRS, grant no. 1.E077.19). Noa Ligot is grateful to VOCATIO for the Fonds Ernest Solvay award that contributed to supporting this study. This work was partly funded by a UCLouvain FSR-ARC Talos research grant (grant no. 20/25-106). Noa Ligot and Pierre Delmelle are indebted to Marc Migon (SEFY, Earth and Life Institute) for technical assistance, Xavier Draye (Earth and Life Institute) for lending the camera equipment, and Karen Fontijn (Department of Geosciences, Environment and Society, Université Libre de Bruxelles) for access to the ash-sieving facility.

Financial support. This research has been supported by the FSR-FNRS (Fonds National de la Recherche Scientifique, grant no. 1.E077.19), VOCATIO (Fonds Ernest Solvay award), UCLouvain FSR-ARC ("Talos", grant no. 20/25-106), UCLouvain ("Fonds d'intervention SST pour l'Open Access"), and Assucopie ("Bourse d'aide aux publications pédagogiques en scientifique").

Review statement. This paper was edited by Amy Donovan and reviewed by two anonymous referees.

References

Al Mamun Hossain, S. A., Lixue, W., Chen, T., and Li, Z.: Leaf area index assessment for tomato and cucumber growing period under different water treatments, Plant Soil Environ., 63, https://doi.org/10.17221/568/2017-PSE, 2017.

Arnalds, O.: The influence of volcanic tephra (ash) on ecosystems, in: Adv. Agron., edited by: Sparks, D. L., Academic Press, 331–380, https://doi.org/10.1016/B978-0-12-407685-3.00006-2, 2013.

Ayris, P. M. and Delmelle, P.: The immediate environmental effects of tephra emission, B. Volcanol., 74, 1905–1936, https://doi.org/10.1007/s00445-012-0654-5, 2012.

Bagheri, G. and Bonadonna, C.: Chapter 2 – Aerodynamics of volcanic particles: characterization of size, shape, and settling velocity, in: Volcanic Ash, edited by: Mackie, S., Cashman, K., Ricketts, H., Rust, A., and Watson, M., Elsevier, 39–52, https://doi.org/10.1016/B978-0-08-100405-0.00005-7, 2016.

Benson, H. and Benson, H. (Ed.): Physique I: Mécanique, 5th edn., De Boeck Supérieur, ISBN 9782761354998, 2015.

Bhushan, B. and Jung, Y. C.: Micro- and nanoscale characterization of hydrophobic and hydrophilic leaf surfaces, Nanotechnology, 17, 2758, https://doi.org/10.1088/0957-4484/17/11/008, 2006.

Biass, S., Jenkins, S. F., Aeberhard, W. H., Delmelle, P., and Wilson, T.: Insights into the vulnerability of vegetation to tephra fallouts from interpretable machine learning and big Earth observation data, Nat. Hazards Earth Syst. Sci., 22, 2829–2855, https://doi.org/10.5194/nhess-22-2829-2022, 2022.

Bilderback, D. E.: Mount St. Helens 1980: botanical consequences of the explosive eruptions, University of California Press, ISBN 0520056086, 1987.

Biscoe, P. V., Gallagher, J. N., Landsberg, J. J., and Cutting, C. V.: Weather, dry matter production and yield, in: Environmental Effects on Crop Physiology, edited by: Landsberg, J. J. and Cutting, C. V., Academic Press, London, 75–100, https://agris.fao.org/agris-search/search.do?recordID=US201302407787 (last access: 30 March 2023), 1977.

Blake, D. M., Hayes, J. L., Andreastuti, S., Hendrasto, M., Wilson, G., Jenkins, S. F., Daniswara, R., Cronin, S., Stewart, C., Wilson, T. M., Ferdiwijaya, D., Craig, H. M., Horwell, C. J., and Leonard, G. S.: The 2014 eruption of Kelud volcano, Indonesia: impacts on infrastructure, utilities, agriculture and health, GNS Science, New Zealand, 130 pp., https://www.researchgate.net/publication/312580340_The_2014_eruption_of_Kelud_volcano_Indonesia_impacts_on_infrastructure_utilities_agriculture_and_health (last access: 24 August 2022), 2015.

Blong, R.: The effects on agriculture, in: Volcanic Hazards: a sourcebook on the effects of eruptions, Academic Press, London, 311–350, https://doi.org/10.1016/0166-3097(86)90025-8, 1984.

Brown, S. K., Auker, M. R., and Sparks, R. S. J.: Populations around Holocene volcanoes and development of a Population Exposure Index, in: Global Volcanic Hazards and Risk, edited by: Vye-Brown, C., Brown, S. K., Sparks, S., Loughlin, S. C., and Jenkins, S. F., Cambridge University Press, Cambridge, 223–232, https://doi.org/10.1017/CBO9781316276273.006, 2015.

Burket, S. D., Furlow, E. P., Golding, P. R., Grant, L. C., Lipovsky, W. A., and Lopp, T. G.: The economic effects of the eruptions of Mt. St. Helens, United States International Trade Commission, Washington, D. C., 20438, 84 pp., USITC Publication 1096, 1980.

Campillo, C., García, M. I., Daza, C., and Prieto, M. H.: Study of a non-destructive method for estimating the leaf area index in vegetable crops using digital images, HortScience, 45, 1459–1463, https://doi.org/10.21273/hortsci.45.10.1459, 2010.

Chamberlain, A. C.: Transport of Lycopodium spores and other small particles to rough surfaces, P. Roy. Soc. Lond. A Mat., 296, 45–70, https://doi.org/10.1098/rspa.1967.0005, 1967.

Chamberlain, A. C. and Chadwick, R. C.: Deposition of spores and other particles on vegetation and soil, Ann. Appl. Biol., 71, 141–158, https://doi.org/10.1111/j.1744-7348.1972.tb02949.x, 1972.

Coltelli, M., Miraglia, L., and Scollo, S.: Characterization of shape and terminal velocity of tephra particles erupted during the 2002 eruption of Etna volcano, Italy, B. Volcanol., 70, 1103–1112, https://doi.org/10.1007/s00445-007-0192-8, 2008.

Cook, R. J., Barron, J. C., Papendick, R. I., and Williams, G. J.: Impact on agriculture of the mount St. Helens eruptions, Science, 211, 16–22, https://doi.org/10.1126/science.211.4477.16, 1981.

Costa, A., Pioli, L., and Bonadonna, C.: Assessing tephra total grain-size distribution: insights from field data analysis, Earth Planet. Sc. Lett., 443, 90–107, https://doi.org/10.1016/j.epsl.2016.02.040, 2016.

Craig, H., Wilson, T., Stewart, C., Outes, V., Villarosa, G., and Baxter, P.: Impacts to agriculture and critical infrastructure in Argentina after ashfall from the 2011 eruption of the Cordón Caulle volcanic complex: an assessment of published damage and function thresholds, J. Appl. Volcanol., 5, 7, https://doi.org/10.1186/s13617-016-0046-1, 2016a.

Craig, H., Wilson, T., Stewart, C., Villarosa, G., Outes, V., Cronin, S., and Jenkins, S.: Agricultural impact assessment and management after three widespread tephra falls in Patagonia, South America, Nat. Hazards, 82, 1167–1229, https://doi.org/10.1007/s11069-016-2240-1, 2016b.

Craig, H., Wilson, T., Magill, C., Stewart, C., and Wild, A. J.: Agriculture and forestry impact assessment for tephra fall hazard: fragility function development and New Zealand scenario application, Volcanica, 4, 345–367, https://doi.org/10.30909/vol.04.02.345367, 2021.

Craig, H. M.: Agricultural vulnerability to tephra fall impacts, Geology, University of Canterbury, Canterbury, 375 pp., https://doi.org/10.26021/6184, 2015.

Darge, A., Sharma, R. D. R., Zerihum, D., and Chung, P. Y. K.: Multi color image segmentation using L*A*B* color space, International Journal of Advanced Engineering, Management and Science, 5, 346–352, https://doi.org/10.22161/IJAEMS.5.5.8, 2019.

de Guzman, E. M.: The Pinatubo eruption of June 1991: the nature and impact of the disaster, Asian Disaster Reduction Center, https://reliefweb.int/report/philippines/eruption-mount-pinatubo-philippines-june-1991 (last access: 31 July 2022), 2005.

Dellino, P., Mele, D., Bonasia, R., Braia, G., La Volpe, L., and Sulpizio, R.: The analysis of the influence of pumice shape on its terminal velocity, Geophys. Res. Lett., 32, 1–4, https://doi.org/10.1029/2005gl023954, 2005.

Eggler, W. A.: Plant communities in the vicinity of the volcano El Paricutin, Mexico, after two and a half years of eruption, Ecology, 29, 415–436, https://doi.org/10.2307/1932635, 1948.

Elia, A. and Conversa, G.: Agronomic and physiological responses of a tomato crop to nitrogen input, Eur. J. Agron., 40, 64–74, https://doi.org/10.1016/j.eja.2012.02.001, 2012.

Eychenne, J., Le Pennec, J.-L., Troncoso, L., Gouhier, M., and Nedelec, J.-M.: Causes and consequences of bimodal grain-size distribution of tephra fall deposited during the August 2006 Tungurahua eruption (Ecuador), B. Volcanol., 74, 187–205, https://doi.org/10.1007/s00445-011-0517-5, 2012.

Fang, H., Frederic, B., Plummer, S., and Schaepman-Strub, G.: An overview of global leaf area Index (LAI): methods, products, validation, and applications, Rev. Geophys., 57, 739–799, https://doi.org/10.1029/2018RG000608, 2019.

FAO (Food and Agriculture Organisation): The impact of disasters and crises on agriculture and food security: 2021, Rome, 245 pp., https://doi.org/10.4060/cb3673en, 2021.

Fierstein, J. and Nathenson, M.: Another look at the calculation of fallout tephra volumes, B. Volcanol., 54, 156–167, https://doi.org/10.1007/BF00278005, 1992.

Freire, S., Florczyk, A. J., Pesaresi, M., and Sliuzas, R.: An improved global analysis of population distribution in proximity to active volcanoes, 1975–2015, ISPRS Int. J. Geo-inf., 8, 341, https://doi.org/10.3390/ijgi8080341, 2019.

Gregory, P. H.: The microbiology of the atmosphere, 1st edn., L. Hill, London, https://doi.org/10.5962/bhl.title.7291, 1961.

Grishin, S. Y., del Moral, R., Krestov, P. V., and Verkholat, V. P.: Succession following the catastrophic eruption of Ksudach volcano (Kamchatka, 1907), Vegetatio, 127, 129–153, https://doi.org/10.1007/BF00044637, 1996.

Hatfield, J.: Radiation use efficiency: evaluation of cropping and management systems, Agron. J., 106, 1820, https://doi.org/10.2134/agronj2013.0310, 2014.

Hay, R. K. M.: Harvest index: A review of its use in plant breeding and crop physiology, Ann. Appl. Biol., 126, 197–216, https://doi.org/10.1111/j.1744-7348.1995.tb05015.x, 2008.

Hay, R. K. M. and Porter, J. R.: The physiology of crop yield, 2nd edn., Blackwell Publishing, 314 pp., https://doi.org/10.1017/S0014479707005595, 2006.

Hirano, T., Kiyota, M., Kitaya, Y., and Aiga, I.: The physical effects of dust on photosynthetic rate of plant leaves, J. Agric. Meteorol., 46, 1–7, https://doi.org/10.2480/agrmet.46.1, 1990.

Hirano, T., Kiyota, M., and Aiga, I.: The effects of dust by covering and plugging stomata and by increasing leaf temperature on photosynthetic rate of plant leaves, J. Agric. Meteorol., 46, 215–222, https://doi.org/10.2480/agrmet.46.215, 1991.

Hirano, T., Kiyota, M., Seki, K., and Aiga, I.: Effects of volcanic ashes from Mt. Unzen-Fugendake and Mt. Sakurajima on leaf temperature and stomatal conductance of cucumber, J. Agric. Meteorol., 48, 139–145, https://doi.org/10.2480/agrmet.48.139, 1992.

Hirano, T., Kiyota, M., and Aiga, I.: Physical effects of dust on leaf physiology of cucumber and kidney bean plants, Environ. Pollut., 89, 255–261, https://doi.org/10.1016/0269-7491(94)00075-O, 1995.

Hosseini, M., McNairn, H., Merzouki, A., and Pacheco, A.: Estimation of Leaf Area Index (LAI) in corn and soybeans using multi-polarization C- and L-band radar data, Remote Sens. Environ., 170, 77–89, https://doi.org/10.1016/j.rse.2015.09.002, 2015.

Israelachvili, J. N.: Intermolecular and surface forces, 3rd edn., edited by: Burlington, U., Academic Press, Burlington, MA, ISBN: 9780080923635, 2011.

Jenkins, S. F., Spence, R. J. S., Fonseca, J. F. B. D., Solidum, R. U., and Wilson, T. M.: Volcanic risk assessment: quantifying physical vulnerability in the built environment, J. Volcanol. Geoth. Res., 276, 105–120, https://doi.org/10.1016/j.jvolgeores.2014.03.002, 2014.

Jenkins, S. F., Wilson, T. M., Magill, C. R., Miller, V., Stewart, C., Marzocchi, W., and Boulton, M.: Volcanic ash fall hazard and risk: technical background paper for the UNISDR Global Assessment Report on Disaster Risk Reduction 2015, Global Volcano Model and IAVCEI, 43 pp., https://ir.canterbury.ac.nz/bitstream/handle/10092/10551/12649572_GVMc.%20Global%20Volcanic%20Hazards%20and%20Risk%20Technical%20background%20paper%20on%20volcanic%20ash%20fall%20hazard%20and%20risk..pdf?sequence=1&isAllowed=y (last access: 29 October 2021), 2015.

Jenkins, S. F., Biass, S., Williams, G. T., Hayes, J. L., Tennant, E., Yang, Q., Burgos, V., Meredith, E. S., Lerner, G. A., Syarifuddin, M., and Verolino, A.: Evaluating and ranking Southeast Asia's exposure to explosive volcanic hazards, Nat. Hazards Earth Syst. Sci., 22, 1233–1265, https://doi.org/10.5194/nhess-22-1233-2022, 2022.

Johnson, J. E. and Lovaas, A. I.: Progress report on simulated fallout studies, Colorado State University, https://apps.dtic.mil/sti/citations/AD0695683 (last access: 30 March 2023), 1969.

Kemanian, A. R., Stöckle, C. O., Huggins, D. R., and Viega, L. M.: A simple method to estimate harvest index in grain crops, Field Crop. Res., 103, 208–216, https://doi.org/10.1016/j.fcr.2007.06.007, 2007.

Kleinhenz, V., Katroschan, K.-U., Schütt, F., and Stützel, H.: Biomass accumulation and partitioning of tomato under protected cultivation in the humid tropics, Eur. J. Hortic. Sci., 71, 173–182, 2006.

Klepper, B., Rickman, R. W., and Peterson, C. M.: Quantitative characterization of vegetative development in small cereal grains, Agron. J., 74, 789–792, https://doi.org/10.2134/agronj1982.00021962007400050005x, 1982.

Le Guern, F., Bernard, A., and Chevrier, R. M.: Soufrière of guadeloupe 1976–1977 eruption – mass and energy transfer and volcanic health hazards, B. Volcanol., 43, 577–593, https://doi.org/10.1007/BF02597694, 1980.

Le Pennec, J.-L., Ruiz, G. A., Ramón, P., Palacios, E., Mothes, P., and Yepes, H.: Impact of tephra falls on Andean communities: the influences of eruption size and weather conditions during the 1999–2001 activity of Tungurahua volcano, Ecuador, J. Volcanol. Geoth. Res., 217–218, 91–103, https://doi.org/10.1016/j.jvolgeores.2011.06.011, 2012.

Liang, S., Li, X., and Jindi, W.: Advanced remote sensing: terrestrial information extraction and applications, 1st edn., Elsevier, ISBN 0123859557, 2012.

Ligot, N.: Crop vulnerability to tephra fall in volcanic regions: field, experimental and modelling approaches, Earth and Life Institute, UCLouvain, Belgium, 285 pp., http://hdl.handle.net/2078.1/270724 (last access: 30 March 2023), 2022.

Ligot, N.: R-scipt-LAI-LI-biomass-yield-loss, Zenodo [code], https://doi.org/10.5281/zenodo.7781693, 2023a.

Ligot, N.: ImageJ-macro, Zenodo [code], https://doi.org/10.5281/zenodo.7781728, 2023b.

Ligot, N., Guevara, C. A., and Delmelle, P.: Drivers of crop impacts from tephra fallout: insights from interviews with farming communities around Tungurahua volcano, Ecuador, Volcanica, 5, 163–181, https://doi.org/10.30909/vol.05.01.163181, 2022.

Mack, R. N.: Initial effects of ashfall from mount St. Helens on vegetation in eastern Washington and adjacent Idaho, Science, 213, 537–539, https://doi.org/10.1126/science.213.4507.537, 1981.

Magill, C., Wilson, T., and Okada, T.: Observations of tephra fall impacts from the 2011 Shinmoedake eruption, Japan, Earth Planets Space, 65, 18, https://doi.org/10.5047/eps.2013.05.010, 2013.

McLaren, K.: XIII – The development of the CIE 1976 (L* a* b*) uniform colour space and colour-difference formula, J. Soc. Dyers Colour., 92, 338–341, https://doi.org/10.1111/j.1478-4408.1976.tb03301.x, 1976.

Mendoza Perez, C., Ojeda, W., Carlos, R., and Flores, H.: Estimation of leaf area index and yield of greenhouse-grown poblano pepper, Ing. Agric. Biosist., 9, 37–50, https://doi.org/10.5154/r.inagbi.2017.04.009, 2017.

Miller, C. F.: The contamination behavior of fallout-like particles ejected by volcano Irazu, Stanford Research Institute, San Francisco, California, MU-5779, 61 pp., https://apps.dtic.mil/sti/citations/AD0634901 (last access: 19 August 2021), 1966.

Miller, C. F.: Operation ceniza-arena: The retention of fallout particles from volcan Irazu (Costa Rica) by plant and people. Part 2, Stanford Research Institute, San Francisco, California, MU-4890, 247 pp., https://apps.dtic.mil/sti/citations/AD0673202 (last access: 19 August 2021), 1967.

Monte, J. A., de Carvalho, D. F., Medici, L. O., da Silva, L. D. B., and Pimentel, C.: Growth analysis and yield of tomato crop under different irrigation depths, Rev. Bras. Eng. Agr. Amb., 17, 926–931, https://doi.org/10.1590/S1415-43662013000900003, 2013.

Monteith, J. L.: Light Interception and radiative exchange in crop stands, in: Physiological Aspects of Crop Yield, edited by: Easton, J. D., Haskins, F. A., Sullivan, C. Y., and van Bavel, C. H. M., American Society of Agronomy, Wisconsin, 89–115, https://doi.org/10.2135/1969.physiologicalaspects.c9, 1969.

Monteith, J. L.: Solar radiation and productivity in tropical ecosystems, J. Appl. Ecol., 9, 747–766, https://doi.org/10.2307/2401901, 1972.

Monteith, J. L.: Climate and the efficiency of crop production in Britain, Philos. T. Roy. Soc. B, 281, 277–294, 1977.

Neild, J., O'Flaherty, P., Hedley, P., Underwood, R., Johnston, D., Christenson, B., and Brown, P.: Impact of a volcanic eruption on agriculture and forestry in New Zealand, Ministry of Agriculture and Forestry, New Zealand, 99/2, 88 pp., https://www.mpi.govt.nz/dmsdocument/138/direct (last access: 19 August 2021), 1998.

Neslon, G. L. M.: Land rehabilitation techniques of rice farmers in Pampanga (Philippines) after the Mt. Pinatubo eruption, Asia Life Sci., 22, 155–181, 2013.

Newhall, C. G. and Self, S.: The volcanic explosivity index (VEI): an estimate of explosive magnitude for historical volcanism, J. Geophys. Res., 87, 1231–1238, https://doi.org/10.1029/JC087iC02p01231, 1982.

Niklas, K. J.: A mechanical perspective on foliage leaf form and function, New Phytol., 143, 19–31, https://doi.org/10.1046/j.1469-8137.1999.00441.x, 1999.

Nurfiani, D. and Bouvet de Maisonneuve, C.: Furthering the investigation of eruption styles through quantitative shape analyses of volcanic ash particles, J. Volcanol. Geoth. Res., 354, 102–114, https://doi.org/10.1016/j.jvolgeores.2017.12.001, 2017.

Onofri, A.: The broken bridge between biologists and statisticians: A blog and R package, https://github.com/OnofriAndreaPG/aomisc (last access: 2 February 2022), 2020.

Pinheiro, J. and Bates, D.: Package "nlme". The Comprehensive R Archive Network, https://cran.r-project.org/web/packages/nlme/nlme.pdf, last access: 31 July 2022.

Poorter, H., Jagodziński, A., Ruiz-Peinado, R., Kuyah, S., Luo, Y., Oleksyn, J., Usol'tsev, V., Buckley, T., Reich, P., and Sack, L.: How does biomass distribution change with size and differ among species? An analysis for 1200 plant species from five continents, New Phytol., 208, 736–749, https://doi.org/10.1111/nph.13571, 2015.

Ram, S. S., Majumder, S., Chaudhuri, P., Chanda, S., Santra, S. C., Maiti, P. K., Sudarshan, M., and Chakraborty, A.: Plant canopies: bio-monitor and trap for re-suspended dust particulates contaminated with heavy metals, Mitig. Adapt. Strat. Gl., 19, 499–508, https://doi.org/10.1007/s11027-012-9445-8, 2012.

Rosso, P., Nendel, C., Gilardi, N., Udroiu, C., and Chlébowski, F.: Processing of remote sensing information to retrieve leaf area index in barley: a comparison of methods, Precis. Agric., 23, 1449–1472, https://doi.org/10.1007/s11119-022-09893-4, 2022.

Rust, A. and Cashman, K.: Permeability controls on expansion and size distributions of pyroclasts, J. Geophys. Res.-Sol. Ea., 116, 1–17, https://doi.org/10.1029/2011JB008494, 2011.

Sæbø, A., Popek, R., Nawrot, B., Hanslin, H. M., Gawronska, H., and Gawronski, S. W.: Plant species differences in particulate matter accumulation on leaf surfaces, Sci. Total Environ., 427–428, 347–354, https://doi.org/10.1016/j.scitotenv.2012.03.084, 2012.

Schindelin, J., Rueden, C. T., Hiner, M. C., and Eliceiri, K. W.: The ImageJ ecosystem: an open platform for biomed-

ical image analysis, Mol. Reprod. Dev., 82, 518–529, https://doi.org/10.1002/mrd.22489, 2015.

Small, C. and Naumann, T.: The global distribution of human population and recent volcanism, Environ. Hazards-UK, 3, 93–109, https://doi.org/10.3763/ehaz.2001.0309, 2001.

Smith, W. H. and Staskawicz, B. J.: Removal of atmospheric particles by leaves and twigs of urban trees: some preliminary observations and assessment of research needs, Environ. Manage., 1, 317–330, https://doi.org/10.1007/BF01865859, 1977.

Solargis: Solar resource maps of Belgium, https://solargis.com/maps-and-gis-data/download/belgium, last access: 17 March 2022.

Starr, J. R.: Inertial impaction of particulates upon bodies of simple geometry, Ann. Occup. Hyg., 10, 349–361, https://doi.org/10.1093/annhyg/10.4.349, 1967.

Sword-Daniels, V., Wardman, J., Stewart, C., Wilson, T., Johnston, D., and Rossetto, T.: Infrastructure impacts, management and adaptations to eruptions at Volcán Tungurahua, Ecuador, 1999–2010, Institute of Geological and Nuclear Sciences, New Zealand, 90 pp., https://ir.canterbury.ac.nz/handle/10092/7135 (last access: 7 February 2022), 2011.

Tabor, D.: Surface forces and surface interactions, J. Colloid Interf. Sci., 58, 3–14, https://doi.org/10.1016/B978-0-12-404501-9.50009-2, 1977.

Tampubolon, J., Nainggolan, H. L., Ginting, A., and Aritonang, J.: Mount Sinabung eruption: Impact on local economy and smallholder farming in KaroRegency, North Sumatra, IOP Conference Series: Earth and Environmental Science, 178, 012039, https://doi.org/10.1088/1755-1315/178/1/012039, 2018.

Tarasenko, I.: Environmental effects of volcanic eruptions: A multidisciplinary study of tephra impacts on plant and soil, Université catholique de Louvain, Belgium, https://dial.uclouvain.be/pr/boreal/object/boreal:203017 (last access: 19 August 2021), 2018.

Thompson, J. R., Mueller, P. W., Flückiger, W., and Rutter, A. J.: The effect of dust on photosynthesis and its significance for roadside plants, Environ. Pollut. Control, 34, 171–190, https://doi.org/10.1016/0143-1471(84)90056-4, 1984.

UNDRO (Office of the United Nations Disaster Relief co-Ordinator): Natural disasters and vulnerability analysis: report of expert group meeting, 9–12 July 1979, UN, Geneva, 48 pp., https://digitallibrary.un.org/record/95986/files/UNDRO_ExpGrp_1-EN.pdf (last access: 16 February 2022), 1980.

Van den Bogaard, P. and Schmincke, H. U.: The eruptive center of the late quaternary Laacher See tephra, Geol. Rundsch., 73, 933–980, https://doi.org/10.1007/BF01820883, 1984.

Vogel, S.: Drag and reconfiguration of broad leaves in high winds, J. Exp. Bot., 40, 941–948, https://doi.org/10.1093/jxb/40.8.941, 1989.

Weraduwage, S. M., Chen, J., Anozie, F. C., Morales, A., Weise, S. E., and Sharkey, T. D.: The relationship between leaf area growth and biomass accumulation in Arabidopsis thaliana, Front. Plant Sci., 6, 167, https://doi.org/10.3389/fpls.2015.00167, 2015.

Wilson, J. W.: Ecological data on dry-matter production by plants and plant communities, in: The Collection and Processing of Field Data, edited by: Bradley, E. F. and Denmead, O. T., Interscience Publishers, New York, USA, 1967.

Wilson, T. M. and Kaye, G. D.: Agricultural fragility estimates for volcanic ash fall hazards, Institute of Geological and Nuclear Sciences, New Zealand, 51 pp., https://www.worldcat.org/title/agricultural-fragility-estimates-for-volcanic-ash-fall-hazards/oclc/217260623 (last access: 18 August 2021), 2007.

Wilson, T. M., Kaye, G., Stewart, C., and Cole, J.: Impacts of the 2006 eruption of Merapi volcano, Indonesia, on agriculture and infrastructure, Institute of Geological and Nuclear Sciences, New Zealand, 64 pp., http://hdl.handle.net/10092/760 (last access: 30 March 2023), 2007.

Wilson, T. M., Cole, J., Cronin, S., Stewart, C., and Johnston, D.: Impacts on agriculture following the 1991 eruption of Vulcan Hudson, Patagonia: lessons for recovery, Nat. Hazards, 57, 185–212, https://doi.org/10.1007/s11069-010-9604-8, 2011.

Witherspoon, J. P. and Taylor Jr., F. G.: Interception and retention of a simulated fallout by agricultural plants, Health Phys., 19, 493–499, https://doi.org/10.1097/00004032-197010000-00003, 1970.

Wohletz, K. H.: Mechanisms of hydrovolcanic pyroclast formation: grain-size, scanning electron microscopy, and experimental studies, J. Volcanol. Geoth. Res., 17, 31–63, https://doi.org/10.1016/0377-0273(83)90061-6, 1983.

Zhang, W., Wang, B., and Niu, X.: Relationship between leaf surface characteristics and particle capturing capacities of different tree species in Beijing, Forests, 8, 92, https://doi.org/10.3390/f8030092, 2017.